Am J Cancer Res 2022;12(3):1116-1128
www.ajcr.us /ISSN:2156-6976/ajcr0138641

Original Article

Multicellular tumor spheroids of LNCaP-Luc prostate cancer cells as *in vitro* screening models for cytotoxic drugs

Elodie Jouberton[1], Aurélien Voissiere[2], Frédérique Penault-Llorca[1], Florent Cachin[1], Elisabeth Miot-Noirault[2]

[1]Clermont Auvergne University, Centre Jean Perrin, INSERM, U1240 Molecular Imaging and Theranostic Strategies, F-63000 Clermont Ferrand, France; [2]Clermont Auvergne University, INSERM, U1240 Molecular Imaging and Theranostic Strategies, F-63000 Clermont Ferrand, France

Received August 27, 2021; Accepted November 22, 2021; Epub March 15, 2022; Published March 30, 2022

Abstract: An increasing number of studies concerning solid cancers, including prostate cancer, are tending to demonstrate the predominant role of the interactions of tumor cells with their microenvironment, and underlining the relevance of therapeutic approaches co-targeting these two components. Artificial *in vitro* 3D culture models, such as spheroids, are therefore being designed to allow intercellular interactions between tumor cells and the matrix, under hypoxic conditions mimicking a microtumor. This project aims to develop and characterize a multicellular tumor spheroid (MCTS) model of human prostate cancer cells expressing PSMA, for *in vitro* drug screening. To this end, 1,000 cells/well were seeded in 100 µl of culture medium with 0.5% of methylcellulose in 96-well, non-adherent, V-shaped bottom plates. Bioluminescent imaging of the spheroids enabled the measurement of spheroid growth. From Day 7 of growth, immunofluorescence studies showed cellular proliferation (Ki-67), mainly located in the periphery of the spheroid section, associated with the formation of an apoptotic core (TUNEL). Scanning electron microscopy and fluorescent imaging (Lox-1 probe) showed the presence of an extracellular matrix and the installation of an oxygen gradient leading to the formation of a hypoxic area during growth. This hypoxia was correlated with increased VEGF excretion. Drug sensitivity was assessed on 2D and 3D cultures. The LNCaP-Luc spheroids are more resistant to docetaxel and TH-302, a hypoxia-activated prodrug, compared with cells grown in a monolayer. For docetaxel, this resistance increased with the spheroid growth stage, whereas the activity of TH-302 was potentiated by the hypoxic environment. In conclusion, the development of LNCaP-Luc cell MCTS provides a simple model mimicking a microtumor; it appears to be particularly well-suited to the validation of new therapeutic approaches targeting proliferation and the microenvironment.

Keywords: Prostate cancer, spheroid, hypoxia

Introduction

Hypoxia is a hallmark of solid tumors in humans, including prostate cancer, that contributes directly to tumor progression [1]. Several studies have shown the presence of moderate to severe hypoxia areas or even anoxia in a wide variety of human tumors (breast cancer, uterine cervix, soft tissue sarcomas, prostate cancer, etc.) [2-5]. Considering oxygen concentration in solid tumors, several authors have noted high heterogeneity between patients as well as within actual tumor tissue during disease progression and in response to therapy [6-9]. Neovascularisation is anarchic and permeable, with an abnormal structure (fenestrations, absence of basal membranes) and functions; this leads to variable and chaotic blood flow causing hypoxic areas and tumor acidification [9]. In cancer patients, tumor hypoxia is associated with a poor prognosis. Hypoxia increases tumor malignancy, promotes resistance to chemo-, radio- and immune-therapies and favors metastatic development [10-12]. Furthermore, hypoxia confers resistance to conventional therapies by modulating the expression of HIF-1α-regulated genes, contributing to a Multi Drug Resistance (MDR) phenotype [13, 14]. The low level of oxygen in hypoxic cells limits the production of reactive oxygen species

(ROS) during radiotherapy, leading to tumor radioresistance [15, 16]. In order to improve the therapeutic response of patients, many teams are working to develop new therapies to target tumor cells specifically located in hypoxic areas, in addition to conventional therapies that are more effective against normoxic cells [17, 18].

Monolayer cell cultures have been the reference model for screening new therapeutic molecules for many decades; so far, multiple discrepancies have been observed between the results obtained *in vitro* and *in vivo*. Several factors may be involved in the anarchic arrangement of cells in the tumor tissue, compared with the orderly arrangement of monolayer culture cells, such as the absence of oxygen, nutrient and proliferation gradient in the tumors and the lack of consideration of cell-cell and cell-extracellular-matrix interactions [19]. It has therefore become essential to develop more appropriate *in vitro* models, such as 3D cell culture models, that better reproduce the ecosystem of the tumor for drug screening, by mimicking the tissue architecture and cell-matrix interactions [20-22]. Such models include long-known multicellular spheroids as well as more recent and sophisticated developments, such as organotypic cultures and organoids, organ-on-a-chip, and 3D bioprinted tissues [23-26]. Regarding hypoxia, the configuration of 3D models offers the advantage of the outer layer of cells being the only cells to interact directly with the medium, simulating tumor hypoxia in tumor areas not reached by blood vessels [27]. For prostate cancer, it has been demonstrated that a hypoxic and acidic microenvironment is correlated with aggressiveness and tumor development, particularly for castration-resistant progression, and could prevent drug diffusion, thus promoting therapeutic resistance [28-31].

In this context, we have developed and characterized a 3D spheroid model of human prostate cancer LNCaP-Luc cells as a tool for *in vitro* drug screening. We specifically performed longitudinal monitoring of morphological parameters and biomarkers expressing hypoxia, apoptosis, vascularization, and prostate cancer antigen (PCA) during spheroid growth. The response of the LNCaP-Luc spheroids to the hypoxia-activated prodrug TH-302 (Evofosfamide) and to conventional chemotherapeutic drugs (docetaxel) was also determined and compared with monolayer cell cultures.

Materials and methods

Cell lines and spheroid culture

LNCaP-Luc human prostate cancer cell lines were purchased from Perkin Elmer (Villebon sur Yvette, France), cultured in RPMI 1640 medium (Gibco®) supplemented with 10% fetal calf serum (Dutscher, Brumath, France) and 4 µg/mL gentamycin (PANTMBiotech). The cells were maintained at 37°C in a humidified atmosphere containing 5% CO_2 and 21% O_2.

For spheroid formation, the LNCaP-Luc cells were seeded in 96-well, non-adherent plates (Nunc) at a density of 250 to 2,000 cells/well in 100 µL of 0.5% of methylcellulose (Bio-Techne) diluted in culture medium. The plates were then placed at 37°C in a humidified atmosphere containing 5% CO_2 and 21% O_2.

Spheroid volume determination

The diameters of 8 spheroids were estimated at Day 1 and Day 21 post-seeding from the major (a) and minor (b) axes, measured in mm, using Image J software and applying the following formula: $V\ (mm^3) = a(b^2/2)$.

Scanning electron microscopy

The spheroids (Day 7) were washed (0.2 M sodium cacodylate buffer pH 7.4) and fixed (1.6% glutaraldehyde in 0.2 M sodium cacodylate buffer pH 7.4) overnight at 4°C. They were then rinsed and fixed in 1% osmium tetroxide in 0.2 M sodium cacodylate buffer (pH 7.4) and dehydrated in a series of ethanol baths (25%, 50%, 70%, 95% and 100%). Finally, the spheroids were immersed in hexamethyldisilazane (HMDS) for 10 minutes (twice) at room temperature. For the visualization phase, the samples were mounted on a metal pad using adhesive carbon tabs. A metallization step was then carried out, corresponding to the deposition of a layer of gold/palladium (JFC-1300, Jeol) on the surface of the sample. The samples were then observed using a scanning electron microscope (Jeol 6060-LV) at an acceleration voltage of 5 kV.

Doubling time of LNCaP-Luc in monolayer and spheroid cultures

The monolayer cells were seeded in black-opaque 96-well plates (Corning®) and the spheroids (Day 1 to Day 14) were individually transferred to a black-opaque 96-well plate (Corning®) and incubated with 15 µg Luciferin (PerkinElmer). Imaging was performed 10 minutes after incubation (exposure time of 3 min) for the monolayer cells and after 15 minutes for the spheroids (at least 3 replicates per condition, n=3). For the quantitative analysis, Living Image® Software (Caliper Life Science, United States) was used with a manually-determined region of interest. The spheroid doubling time was then determined by exponential linear regression using Graphpad prism software, using a standard range with the cell line grown in a monolayer.

PSA and VEGF ELISA assays

VEGF (vascular endothelial growth factor) was quantified by Elisa assay on the spheroid medium at Day 5, Day 7 and Day 10 after cell seeding and 72 hours after cell seeding for the monolayer cells using the Elisa "Human VEGF" assay kit (R&D Systems) according to the manufacturer's instructions. Optical density was measured using a Multiskan™ GO instrument (Thermo Scientific).

The PSA (Prostate Specific Antigen) antigen Elisa assay was performed on the spheroid medium at Day 3, Day 7, Day 14 before treatment and 48 hours after treatment, using the "Human Kallikrein 3/PSA (R&D Systems) assay kit" according to the manufacturer's instructions. Optical density was measured using a Multiskan™ GO instrument (Thermo Scientific).

Detection of apoptotic cells by IncuCyte and TUNEL assays

Apoptosis measurement studies were performed only on the spheroids.

For the apoptosis assays, Caspase 3/7 green reagent (IncuCyte, Essen Bioscience) was used according to the manufacturer's instructions. Fluorescence was measured for one hour per day for 14 days after cell seeding and imaged using an IncuCyte imaging system (Essen Bioscience) at 37°C, 5% CO_2. Data were analyzed and quantified using the IncuCyte analysis. Experiments were performed in triplicate.

For the TUNEL assay, the slides were incubated for 1.5 hours at 37°C with a mixture of 20 U/µL TdT (terminal deoxynucleotidyl transferase, Thermo Scientific), 1 mM biotin-11-dUTP (Thermo Scientific) and 1 mM ATP in TdT buffer. After washing, the slides were incubated with streptavidin-HRP (Vector Laboratories, 1/500) at room temperature for 30 minutes. HRP was then detected by tyramide signal amplification according to the manufacturer's instructions (TSA-Alexa555, Invitrogen). The nuclei were counterstained with Hoechst 33342. Fluorescence emission was detected using an Axioplan microscope (Zeiss), and the images were recorded by an AxioCam MRs5 camera (Zeiss).

Assessment of spheroid hypoxia by both Lox-1 imaging and pimonidazole IHC

The hypoxia of the LNCaP-Luc spheroids was characterized at several growth stages: initially for the whole spheroid using the Lox-1 probe and then at slice level using IHC with pimonidazole. The Lox-1 probe is a light-emitting iridium compound. Fluorescence is quenched by the presence of oxygen, which means that the lower the oxygen level, the higher the fluorescence. Spheroids at growth stage Day 1, Day 6 and Day 13 were incubated with 200 µM of Lox-1 hypoxia probe (Scivax) for 24 hours at 37°C, 5% CO_2. The spheroids were then sampled and placed between slides in PBS under bright-field and fluorescence microscopy using an Axioplan microscope (Zeiss). Pimonidazole hydrochloride (Hypoxyprobe) was incubated in the spheroid culture medium at a final concentration of 200 µM for 2 hours before fixation. The spheroids were harvested and fixed in 4% formalin, dehydrated with ethanol, and embedded in paraffin. Serial 5 µm sections were cut and mounted on poly-L-lysine-coated glass microscope slides. After deparaffinization and rehydration, the slides were stained with hematoxylin-eosin (H&E). Antigen retrieval for immunostaining was conducted by incubating the slides in 10 mM boiling citrate buffer (pH 6) with 0.05% Tween (v/v) (30 minutes). After an endogenous peroxidase quench (0.3% H_2O_2; 30 minutes) and saturation (1% BSA/PBS; 1 hour),

the slides were incubated with primary antibody anti-Ki-67 (1:2000, Abcam #15580, room temperature, overnight) rabbit monoclonal antibody, or anti-pimonidazole (1:50, Hypoxyprobe, room temperature, 1 hour) mouse monoclonal antibody, or anti-PSMA (1/100, Diagnostic BioSystems, clone 3E6, room temperature, 30 minutes) mouse monoclonal antibody. Secondary biotinylated goat anti-mouse or anti-rabbit IgG1 antibodies (Vector Laboratories BA-1000, 1/500, 1 hour) were used to detect the primary antibody. Biotin was then complexed with streptavidin-coupled HRP (Vector Laboratories #SA-5004, 1/500, 30 minutes), and HRP was detected using tyramide signal amplification according to the manufacturer's instructions (TSA-Alexa488, Invitrogen). The nuclei were counterstained with Hoechst 33342.

Drug cytotoxicity assays

Alamar Blue cell viability assays were performed to determine the cytotoxic activity of conventional chemotherapy (docetaxel) and the hypoxia-activated prodrug TH-302 for LNCaP-Luc spheroid and monolayer culture cells. For the spheroids, the treatments were initiated at Day 3, Day 7 and Day 14 after cell seeding and 24 hours after the seeding of 5,000 cells per well in 96-well plates for the monolayer cell culture. Docetaxel was diluted in the growing culture medium to obtain a final concentration of 1.56 µM to 200 µM and TH-302 in DMSO was added to the growing culture medium at a final concentration of 2.2 µM to 280 µM (maintaining a final concentration of DMSO of 0.5% v/v). After 72 hours of incubation, cytotoxic activity was expressed as the drug concentration that inhibited cell growth by 50% (IC_{50}). Experiments were performed in triplicate.

Statistical analysis

The data presented in this study are expressed as the mean ± standard deviation (SD); they were statistically analyzed using GraphPad Prism software (version 5.0 GraphPad Software, Inc., San Diego, CA). The statistical difference between the experiment groups was compared using the Mann-Whitney test. *P* was considered statistically significant when <0.05 (*P<0.05, **P<0.01, ***P<0.001).

Results

3D cell culture of LNCaP-Luc cells

The LNCaP-Luc cells were seeded from 250 to 2,000 cells per well in the presence of 0.5% methylcellulose. As illustrated in **Figure 1A**, the cells rapidly aggregated in the middle of the well, forming a spheroid within 24 hours, regardless of the number of cells seeded. A darker core, identified as a "necrotic core", appeared between Days 3 and 14 of culture, depending on the number of seeded cells. The results show an increase in diameter over time up to Day 21 in all growing conditions (**Figure 1B**). For 250, 1,000 and 2,000 cells per well, the spheroid diameters were 0.008±0.005 µm, 0.039±0.023 µm and 0.066±0.019 µm respectively at Day 3 and 0.104±0.007 µm, 0.179±0.049 µm and 0.191±0.035 µm respectively at Day 21. The necrotic core was measured separately and increased during the 21-day period study. At Day 21 after seeding, the necrotic core volume represented 42% of the total volume of the spheroid. This led us to select the culture condition of 1,000 cells per well for the rest of the studies.

Day 7 observation of the LNCaP-Luc spheroids under the scanning electron microscope confirmed the three-dimensional architecture, exhibiting rounded shapes with granular surfaces covered with stacked cells (**Figure 2A**). The cells were strongly juxtaposed with a large extracellular matrix (ECM).

Bioluminescence intensity was quantified on both monolayer and 3D cultures. Bioluminescence intensity was correlated with the cell number (r^2=0.9993), allowing quantification of the cell number in spheroids over time by "in situ" cell counting with no dissociation process (**Figure 2B** and **2C**). The doubling time was calculated as 32.9 hours (95% confidence interval 15.8 to 66.5) for spheroids and 19 hours for the monolayer culture.

Assessment of proliferative and apoptotic cells in LNCaP-Luc spheroids

H&E staining of the LNCaP-Luc spheroids at Day 3, Day 7 and Day 14 showed high cell density with an ordered architecture (**Figure 3A**). Cell density was lower in the center of the

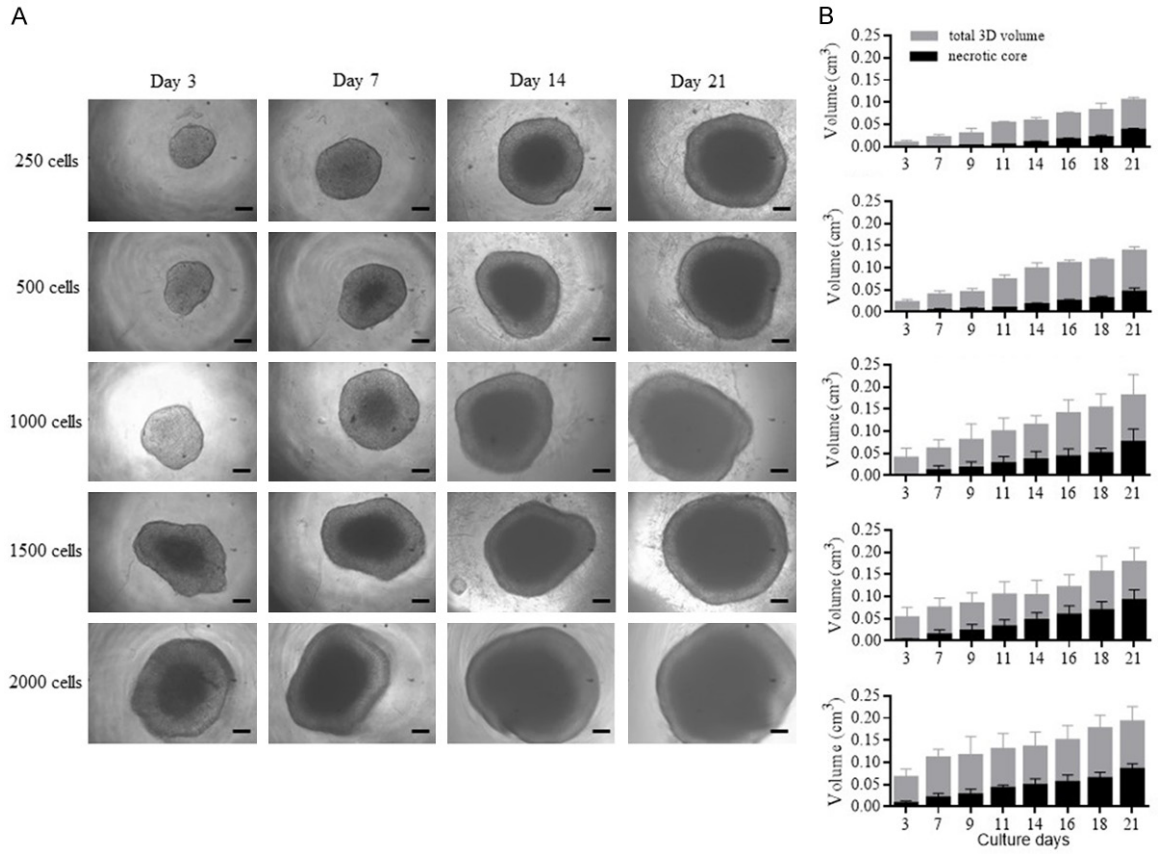

Figure 1. Culture of LNCaP-Luc spheroids. (A) Profile of spheroid formation over time depending on the number of seeded cells. (B) Total 3D volume (grey) and apoptotic core volume (black) of each spheroid measured with Image J software. Major (A) and minor (B) axes measured in mm to calculate volume. Scale bars, 100 µm.

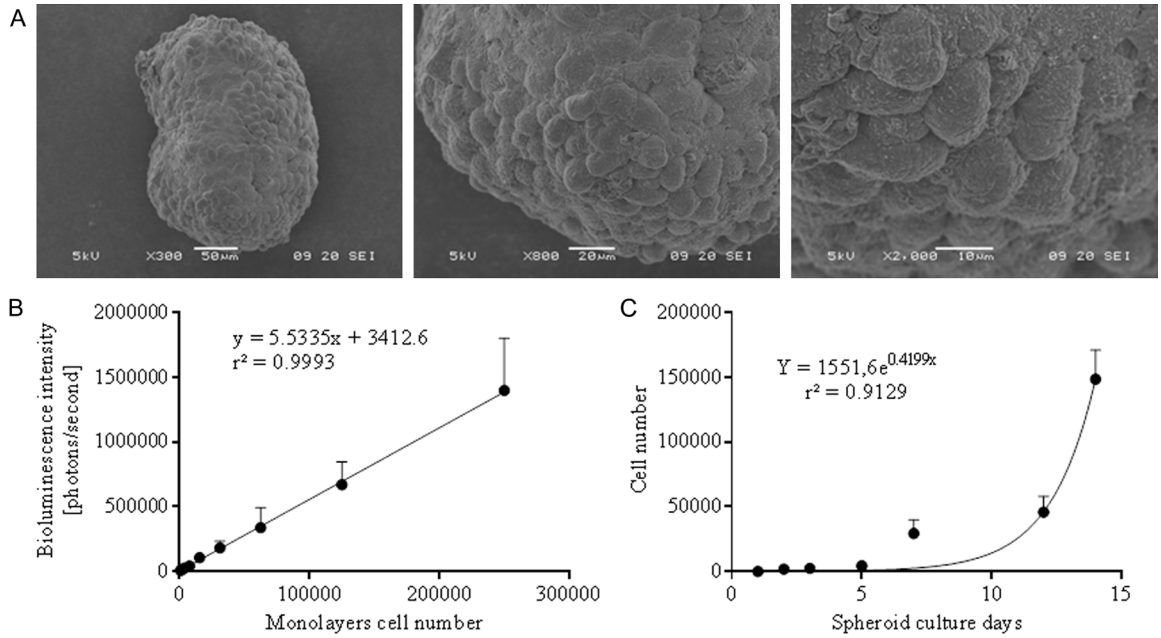

Figure 2. Characterization of LNCaP-Luc spheroid growth. Cells were seeded at 1,000 cells per well. A. SEM images of monocultured spheroids cultured for 7 days. Scale bars, 50 µm. B. Linear quantification of bioluminescent activity with LNCaP-Luc cell number. C. Number of spheroid LNCaP-Luc cells from Days 1 to 14 determined by bioluminescent imaging using the standard curve obtained from monolayer LNCaP-Luc cells.

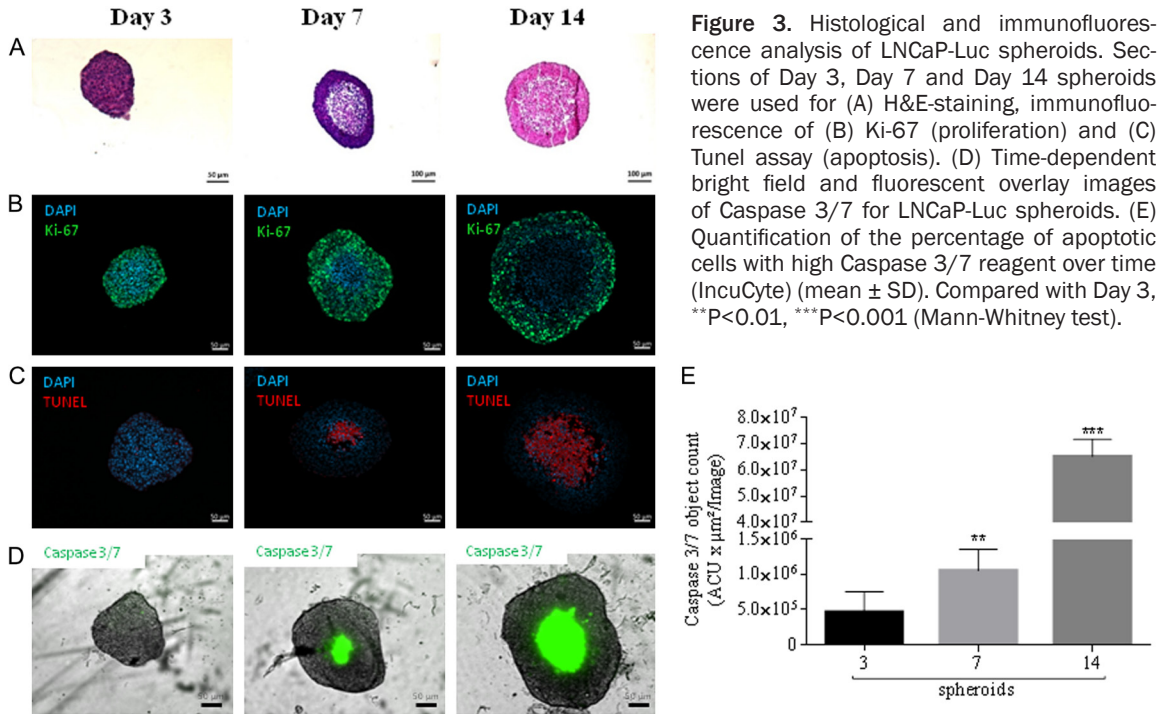

Figure 3. Histological and immunofluorescence analysis of LNCaP-Luc spheroids. Sections of Day 3, Day 7 and Day 14 spheroids were used for (A) H&E-staining, immunofluorescence of (B) Ki-67 (proliferation) and (C) Tunel assay (apoptosis). (D) Time-dependent bright field and fluorescent overlay images of Caspase 3/7 for LNCaP-Luc spheroids. (E) Quantification of the percentage of apoptotic cells with high Caspase 3/7 reagent over time (IncuCyte) (mean ± SD). Compared with Day 3, $^{**}P<0.01$, $^{***}P<0.001$ (Mann-Whitney test).

spheroid section from Day 7, suggesting the establishment of an apoptotic/necrotic area. To confirm this observation, we performed Ki-67 immunohistochemistry to determine the proliferative cells and a TUNEL assay and Caspase 3/7 quantification to identify the dead cells. At Day 3, the proliferative cells (Ki-67 positive, green) were homogenously distributed throughout the section, while at Day 7 and Day 14, the proliferative cells were mainly located on the outskirts of the spheroid (**Figure 3B**). Furthermore, the TUNEL assay and time-lapse imaging of Caspase 3/7 revealed the establishment of an apoptotic core at the center of the spheroids from Day 7 (**Figure 3C-E**), increasing up to Day 14. (Fluorescence intensity of the Caspase 3/7 marker increased from $1.1\times10^6\pm3.0\times10^5$ for Day 7 to $6.5\times10^7\pm6.5\times10^6$ for Day 14). Together, these results suggest that a hypoxic core developed in the spheroids from Day 7 of culture due to an increase in their size, limiting the diffusion of oxygen in the deep layers.

Assessment of prostate tumor biomarkers: PSA and PSMA

To further characterize the prostate LNCaP-Luc spheroids, we focused on the prostate tumor biomarkers currently used in clinical practice (PSA and PSMA). Interestingly, our results indicate that the LNCaP-Luc spheroids secreted PSA from Day 3 of culture, with a significant increase over time, while PSA was not detectable in the monolayer culture (20.1±0.5 at Day 3, 45.8±3.9 and Day 7 and 176.6±4.8 ng/mL at Day 14) (**Figure 4A**).

Moreover, immunofluorescence showed that the prostate membrane antigen (PSMA) biomarker was expressed on the cell surface at an early stage of growth (Day 3 post-seeding) and was maintained, tending to increase throughout the 14 days of culture (**Figure 4B**). These results demonstrate that 3D cell cultures of LNCaP-Luc mimic patient tumors more closely than monolayer cell cultures.

3D cancer cells form a hypoxic core in the scaffold

To confirm that steady state LNCaP-Luc spheroids (from Day 7) exhibit a hypoxic core, we determined VEGF secretion over time using the ELISA assay and measured immunofluorescence using the hypoxia marker pimonidazole and the fluorescent Lox-1 hypoxia probe. As illustrated in **Figure 5A**, from Day 5, the spheroids secreted more VEGF than the monolayer cell cultures (84.0±19.6 vs 46.2±20.3 pg/mL)

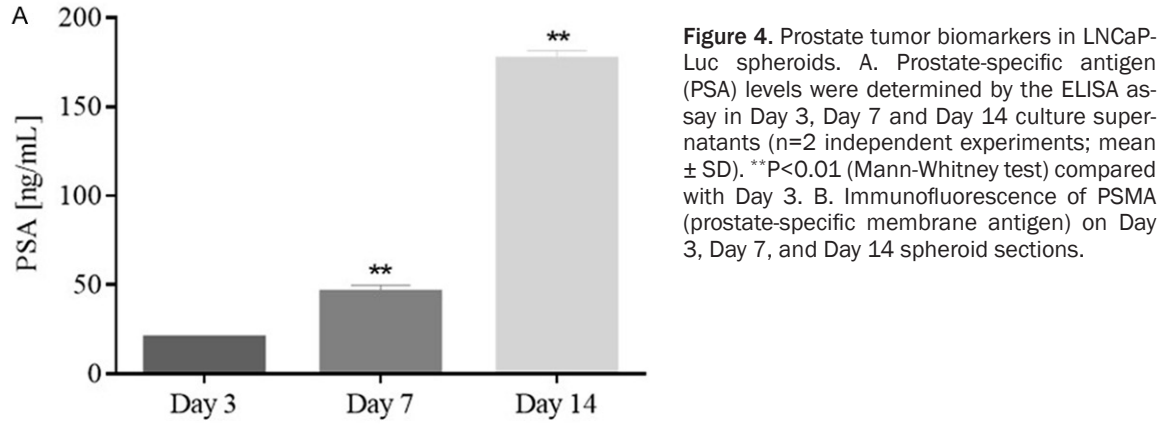

Figure 4. Prostate tumor biomarkers in LNCaP-Luc spheroids. A. Prostate-specific antigen (PSA) levels were determined by the ELISA assay in Day 3, Day 7 and Day 14 culture supernatants (n=2 independent experiments; mean ± SD). **P<0.01 (Mann-Whitney test) compared with Day 3. B. Immunofluorescence of PSMA (prostate-specific membrane antigen) on Day 3, Day 7, and Day 14 spheroid sections.

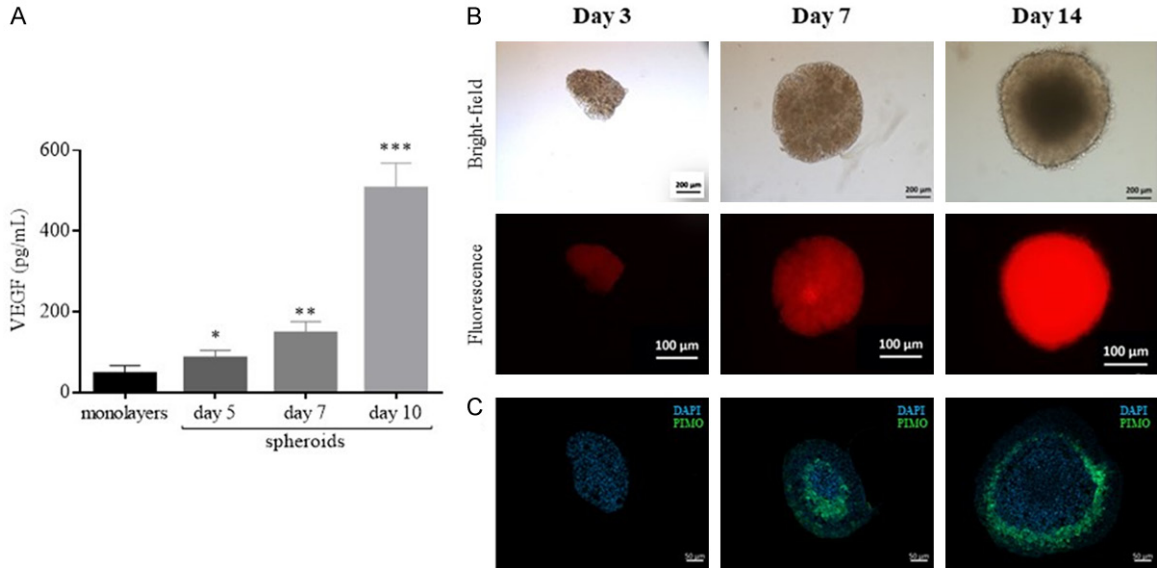

Figure 5. Determination of hypoxia in LNCaP-Luc spheroids. A. VEGF concentration determined by ELISA in monolayer or spheroid culture supernatants (n=3 independent experiments; mean ± SD). *P<0.05, **P<0.01, ***P<0.001 (Mann-Whitney test) compared with monolayers. B. Hypoxic cells detected using LOX-1 hypoxia probe (red). The probe was applied for 24 hours to spheroids before fluorescence detection. C. Determination of hypoxic cells on spheroid sections by immunofluorescence using pimonidazole in Day 3, Day 7 and Day 14 spheroids.

and secretion increased over time. Secretion was significantly higher in Day 10 spheroids (505.6±63.3) (**Figure 5A**). Regarding the hypoxia environment, we observed a stronger fluorescent signal on the Lox-1 hypoxia probe from the spheroids after Day 7 of growth, which

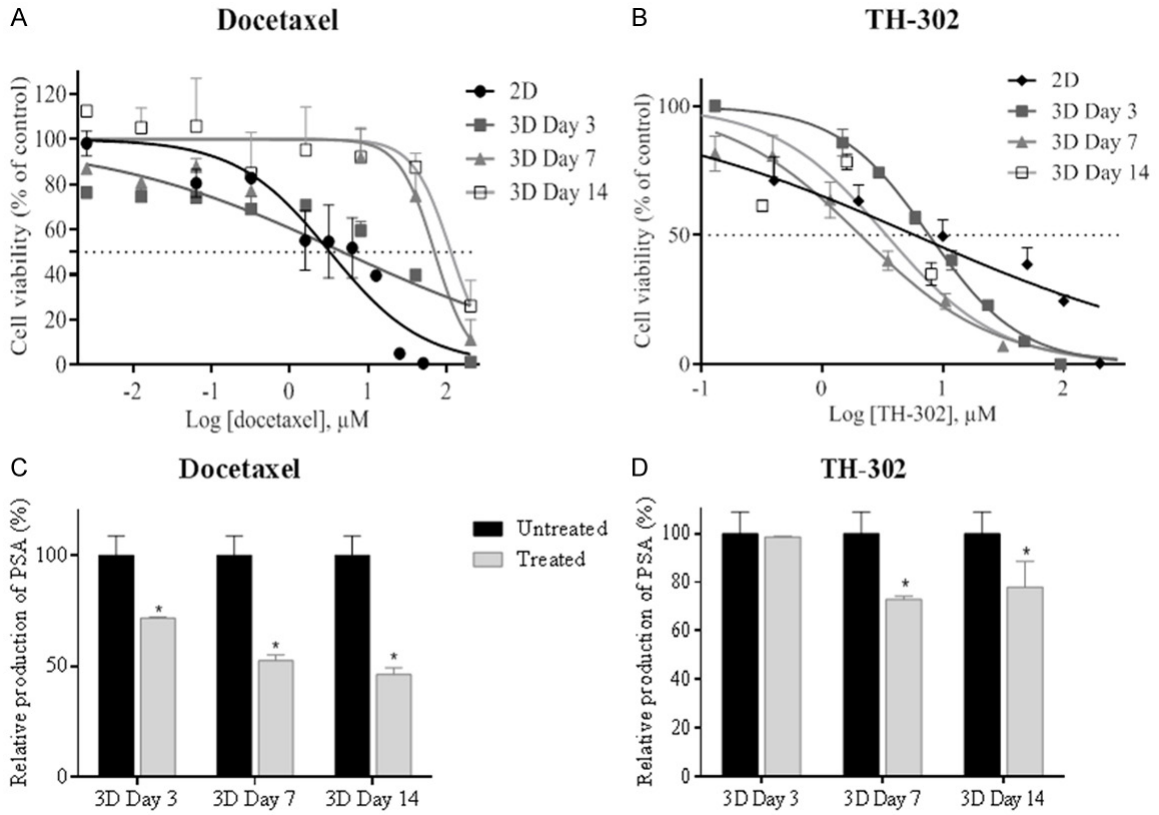

Figure 6. Comparison of cytotoxicity in monolayer cultures and spheroids (3, 7 and 14 culture days) of LNCaP-Luc cells and PSA secretion. Spheroids were exposed to (A) docetaxel and (B) TH-302 following 72 hours of treatment (n=3 replicas; mean ± SD). (C, D) Quantification of PSA production by Day 7 spheroids exposed to IC_{50} of (C) docetaxel or (D) TH-302 for 48 hours. (n=2 replicas; mean ± SD). Compared with untreated, *P<0.05 (Mann-Whitney test).

Table 1. IC_{50} (µM) and multicellular resistance index (MCRI) values for LNCaP-Luc cell cultures (n=3 independent experiments; mean ± SD)

	Docetaxel		TH-302	
	IC_{50} (µM)	MCRI	IC_{50} (µM)	MCRI
Monolayer cells	2.7±1.2	/	7.8±8.3	/
Day 3 spheroid	29.6±9.5	11.1	7.5±6.8	1.0
Day 7 spheroid	57.0±24.9	21.3	1.9±1.7	0.2
Day 14 spheroid	96.0±11.9	36.0	5.5±3.5	0.7

increased significantly at Day 14 (fluorescent with low levels of oxygen) (**Figure 5B**). Pimonidazole immunostaining of the LNCaP-Luc spheroids evidenced a hypoxia area in spheroids from Day 7 to Day 14, but not in Day 3 spheroids (**Figure 5C**). Interestingly, the hypoxia area was located between the surface and the center of Day 7 and Day 14 spheroids, suggesting that the deep central layers of spheroids are necrotic or that the pimonidazole did not diffuse throughout the spheroids (**Figure 5C**). These results demonstrate that the 3D culture of LNCaP-Luc reproduces a hypoxia environment similar to that observed in human tumors.

Drug resistance of hypoxic spheroids and PSA response

We then assessed the cytotoxic activity of a chemotherapeutic regimen used in the clinical treatment of prostate cancer, docetaxel, and of a hypoxia-activated prodrug, TH-302, on LNCaP-Luc cells cultured in a monolayer or cultured in 3D at Day 3, Day 7 and Day 14. The results obtained are shown in **Figure 6** and **Table 1**.

As expected, the spheroids were more resistant to docetaxel than the monolayer cell cultures, and chemoresistance increased as the spheroids grew over time. Indeed, the multicellular resistance index (MCRI) of the spheroids increased from 11.1 at Day 3 to 36.0 at Day 14.

In contrast, hypoxic Day 7 and Day 14 spheroids were more chemosensitive to TH-302 (MCRI of 0.2) and 0.7 respectively, compared with non-hypoxic Day 3 spheroids (MCRI of 1.0) and monolayer cell cultures.

Next, we monitored the therapeutic response of docetaxel and TH-302-treated spheroids by PSA quantification. Surprisingly, PSA secretion decreased significantly over time (71.7±0.5%, 52.6±2.6% and 46.3±3.1% at Days 3, 7 and 14 respectively, P=0.028; **Figure 6C**) during docetaxel treatment, while steady state spheroids (Day 7 and 14) became chemoresistant, suggesting that peripherical cells (normoxia) could be the main source of PSA. Regarding TH-302, PSA secretion decreased slightly at Days 7 and 14 (72.9±1.25% and 77.9±10.7%; P=0.028) compared with Day 3 spheroids (**Figure 6D**).

Together, we demonstrate that LNCaP-Luc cell MCTS, mimicked the biological properties of the tumor microenvironment. MCTS production quantities of VEGF, PSMA and PSA, depended on spheroid development, as well as on cytotoxic treatment used. This model could provide a highly predictive in vitro system for innovative targeted therapies in prostate cancer.

Discussion

Nowadays, the therapeutic strategy of cancer treatment is no longer directed on just the tumor cells but also on the tumor's microenvironment (TME). Mimicking the interactions between tumor cells, stromal cells and extracellular matrix components is critical to further our understanding of the mechanisms underlying the progression of solid tumors and to develop innovative, effective, and safe strategies. This is particularly true for prostate cancer, which is characterized by a highly complex tumor microenvironment, including hypoxic regions, causing significant aggressiveness and resistance to both chemo- and radiotherapies [32].

Drug resistance is an extremely complicated phenomenon that involves several factors. The tumor microenvironment is known to have the ability to induce a resistant phenotype in tumor cells, as well as to obstruct drug delivery by means of blood vessel compression, high interstitial fluid pressure and biomechanical barriers. It is now widely recognized that hypoxia is responsible not only for altering the pharmacokinetics of molecules but also promotes the selection of more resistant cells through a number of signaling pathways related to apoptosis, autophagy, DNA damage, mitochondrial activity, p53, and drug efflux [33]. It is commonly accepted that experimental models could fill the gap between fundamental cancer research and clinical practice if they are able to replicate tumor heterogeneity and the microenvironment of tumors in humans. An ideal model mimicking tumor biology should reproduce the cellular, biochemical and biophysical conditions of tumor tissue, to enable study of the multifaceted features of the multifaceted features of the TME that are responsible for disease progression and resistance to therapy [34]. Monolayer cultures of tumor cells, widely used *in vitro* for cytotoxicity studies, do not take into account tissue architecture, biochemical and biomechanical regulations, or cell-cell and matrix-cell communication [19]. The best compromise to date appears to be the use of spheroid-based models. Some such models are easily standardized and complex enough to represent certain aspects of human tumors, such as microtumor tissue organization, by creating oxygen, nutrient and proliferation gradients during spheroid growth, as well as by mimicking cell-cell and extracellular matrix-cell interactions. Over the past few decades, tumor spheroids have been found to display an organized architecture, combining a layer of proliferative cells and a peripheral area with a central apoptotic and/or necrotic core that limits the diffusion of nutrients, oxygen and drugs throughout the spheroid. Various methods have been used to develop spheroids [25]. MCTS have been optimized and characterized in this study for LNCaP-Luc prostate cancer cells and the model offers the advantage of being scaffold-free, which is considered the best approach for several epithelial cancers, including breast, lung, colorectal and prostate cancers [34]. After seeding 1,000 cells per well in non-adherent multi-well plates, cell interaction was observed from Day 1. As expected, the characterization of LNCaP-Luc spheroids revealed proliferative cells at the periphery of the spheroids, while the central core was characterized by hypoxic and apoptotic areas. Interestingly, with the establishment of hypoxic areas, VEGF was strongly

excreted from Day 5, with a 6-fold increase in production at Day 10. This type of hypoxic zone and the associated VEGF excretion were not obtained in the monolayer cultures. This constitutes a highly relevant characteristic of this new model mimicking *in vivo* conditions. We also demonstrated that the LNCaP-Luc MCTS model was able to reproduce key factors of prostate cancer, such as PSA excretion and expression of the PSMA marker at the cell surface from an early stage of growth (Day 3 post-seeding) with a tendency to increase throughout the 21 days of growth, allowing response monitoring during drug cytotoxic essays. Several previous studies have shown that monolayer cells tend to overestimate the efficacy of chemotherapeutic drugs compared with spheroids [35-37]. Our study provided similar results, showing that 3D cultures are more resistant to standard chemotherapy (docetaxel) compared with monolayer cell cultures. Two main hypotheses can be formulated with regard to this resistance. Firstly, acidification of the microenvironment due to tumor hypoxia modifies the expression of the gene involved in tumor resistance and/or aerobic glycolysis and lactic acid production, lowering the pH (0.6 pH unit); this is known to reduce the uptake of chemotherapeutic drugs by the cancer cells [38]. Indeed, several studies have shown that tumor hypoxia reduces the therapeutic efficacy of certain therapeutic molecules, including anthracyclines, 5-FU and cyclophosphamides [39]. Recently published work reports that hypoxia may induce the resistance of prostate cancer cells to docetaxel [40]. Secondly, 3D conformation of the spheroids generates nutrient, oxygen and catabolite gradients [41]. These conditions, combined with cell-to-cell and cell-to-matrix interactions, could impact gene and protein expression patterns and drug distribution and penetration [25, 42]. In our study, we demonstrated that LNCaP-Luc spheroids are more resistant to docetaxel compared with monolayer cell cultures, with resistance increasing significantly with spheroid growth and the establishment of hypoxia. It was specifically at a late stage of growth (Day 7), when hypoxia was clearly present, that the hypoxia-activated prodrugs, TH-302, demonstrated the highest cytotoxic activity. TH-302 was initially published in 2008 as a hypoxia activated prodrug. TH-302 is a cleavable entity composed of a 2-nitroimidazole moiety linked to a bromo-isophosphoramide mustard (Br-IPM) which, once released, act as a DNA cross linking agent leading to cell cycle arrest [43]. In this work, in vitro cytotoxicity of TH-302 was increased under hypoxic conditions in a panel of 32 human cancer cell lines, and also in 3D tumor spheroid models. In in vivo prostate cancer models, TH-302 has also shown selective toxicity for hypoxic cells but also for the cellular neighbourhood of these hypopoxic cells in tumor tissue [44]. Numerous preclinical and clinical studies exploiting TH-302 in various cancers, have shown its potential in monotherapy or in combination with conventional chemotherapy, with radiotherapy and more recently, in a prostate cancer model, with immunotherapy [45-50]. Therefore, it could be interesting to assess the relevance of combination of TH-302 with docetaxel in our LNCaP-Luc cell MCTS. Considering all the phenotypic features of tumor prostates mimicked by the MCTS culture of LNCaP-Luc cells, it would be interesting to investigate co-cultures with stromal cells, such as fibroblasts, as well as endothelial cells, to get even closer to the *in vivo* environment.

Conclusion

To conclude, we have developed a simple and reproducible MCTS culture model of LNCaP-Luc cells that closely reproduces the features of *in vivo* tumors. This model can be used as an intermediate tool between traditional *in vitro* cell-based assays and *in vivo* models for the high-throughput evaluation of therapeutic candidates; it appears to be particularly relevant for validating new therapeutic approaches targeting proliferation and the microenvironment.

Acknowledgements

We would like to thank Christelle Soubeyrand-Damon (ANIPATH, GReD, Clermont-Ferrand) for her technical assistance with the immunohistochemical studies, Jean-Luc Dubost (chemotherapy preparation unit, Centre Jean Perrin, Clermont-Ferrand) and Christelle Blavignac (CICS, UCA, Clermond-Ferrand) for the scanning electron microscopy. We also express our gratitude to Dr. Valérie Weber (UMR 1240, IMoST, UCA, Clermont-Ferrand) for her support for this project. This work was supported by the Association pour la Recherche sur les Tumeurs de la Prostate (coordinator: Dr V Weber) and

Foncer Contre la Cancer (coordinator: Dr L Mazuel).

Disclosure of conflict of interest

None.

Abbreviations

ECM, extracellular matrix; H&E, hematoxylin-eosin; HMDS, hexamethyldisilazane; IC_{50}, drug concentration that inhibited cell growth by 50%; MCRI, multicellular resistance index; MCTS, multicellular tumor spheroids; MDR, multidrug resistance; PCA, prostate cancer antigen; PSA, prostate-specific antigen; PSMA, prostate membrane antigen; ROS, reactive oxygen species; SD, standard deviation; TME, tumor microenvironment; VEGF, vascular endothelial growth factor.

Address correspondence to: Elodie Jouberton, Clermont Auvergne University, Centre Jean Perrin, INSERM, U1240 Molecular Imaging and Theranostic Strategies, F-63000 Clermont Ferrand, France. Tel: +33-473150804; E-mail: elodie.jouberton@clermont.unicancer.fr

References

[1] Vaupel P, Hockel M and Mayer A. Detection and characterization of tumor hypoxia using pO2 histography. Antioxid Redox Signal 2007; 9: 1221-1235.

[2] Brizel DM, Rosner GL, Harrelson J, Prosnitz LR and Dewhirst MW. Pretreatment oxygenation profiles of human soft tissue sarcomas. Int J Radiat Oncol Biol Phys 1994; 30: 635-642.

[3] Hockel M, Schlenger K, Knoop C and Vaupel P. Oxygenation of carcinomas of the uterine cervix: evaluation by computerized O2 tension measurements. Cancer Res 1991; 51: 6098-6102.

[4] Movsas B, Chapman JD, Hanlon AL, Horwitz EM, Pinover WH, Greenberg RE, Stobbe C and Hanks GE. Hypoxia in human prostate carcinoma: an eppendorf PO2 study. Am J Clin Oncol 2001; 24: 458-461.

[5] Vaupel P, Schlenger K, Knoop C and Hockel M. Oxygenation of human tumors: evaluation of tissue oxygen distribution in breast cancers by computerized O2 tension measurements. Cancer Res 1991; 51: 3316-3322.

[6] Nordsmark M, Bentzen SM and Overgaard J. Measurement of human tumour oxygenation status by a polarographic needle electrode. An analysis of inter- and intratumour heterogeneity. Acta Oncol 1994; 33: 383-389.

[7] Osinsky S, Zavelevich M and Vaupel P. Tumor hypoxia and malignant progression. Exp Oncol 2009; 31: 80-86.

[8] Brahimi-Horn MC, Chiche J and Pouyssegur J. Hypoxia and cancer. J Mol Med (Berl) 2007; 85: 1301-1307.

[9] Harris AL. Hypoxia--a key regulatory factor in tumour growth. Nat Rev Cancer 2002; 2: 38-47.

[10] Khawar IA, Kim JH and Kuh HJ. Improving drug delivery to solid tumors: priming the tumor microenvironment. J Control Release 2015; 201: 78-89.

[11] Vaupel P. Hypoxia and aggressive tumor phenotype: implications for therapy and prognosis. Oncologist 2008; 13 Suppl 3: 21-26.

[12] Vaupel P, Thews O and Hoeckel M. Treatment resistance of solid tumors: role of hypoxia and anemia. Med Oncol 2001; 18: 243-259.

[13] Comerford KM, Wallace TJ, Karhausen J, Louis NA, Montalto MC and Colgan SP. Hypoxia-inducible factor-1-dependent regulation of the multidrug resistance (MDR1) gene. Cancer Res 2002; 62: 3387-3394.

[14] Tezcan O, Ojha T, Storm G, Kiessling F and Lammers T. Targeting cellular and microenvironmental multidrug resistance. Expert Opin Drug Deliv 2016; 13: 1199-1202.

[15] Harrison LB, Chadha M, Hill RJ, Hu K and Shasha D. Impact of tumor hypoxia and anemia on radiation therapy outcomes. Oncologist 2002; 7: 492-508.

[16] Moeller BJ, Richardson RA and Dewhirst MW. Hypoxia and radiotherapy: opportunities for improved outcomes in cancer treatment. Cancer Metastasis Rev 2007; 26: 241-248.

[17] Courtney KD, Infante JR, Lam ET, Figlin RA, Rini BI, Brugarolas J, Zojwalla NJ, Lowe AM, Wang K, Wallace EM, Josey JA and Choueiri TK. Phase I dose-escalation trial of PT2385, a first-in-class hypoxia-inducible factor-2alpha antagonist in patients with previously treated advanced clear cell renal cell carcinoma. J Clin Oncol 2018; 36: 867-874.

[18] Mistry IN, Thomas M, Calder EDD, Conway SJ and Hammond EM. Clinical advances of hypoxia-activated prodrugs in combination with radiation therapy. Int J Radiat Oncol Biol Phys 2017; 98: 1183-1196.

[19] Chambers KF, Mosaad EM, Russell PJ, Clements JA and Doran MR. 3D cultures of prostate cancer cells cultured in a novel high-throughput culture platform are more resistant to chemotherapeutics compared to cells cultured in monolayer. PLoS One 2014; 9: e111029.

[20] Han SJ, Kwon S and Kim KS. Challenges of applying multicellular tumor spheroids in preclinical phase. Cancer Cell Int 2021; 21: 152.

[21] Voissiere A, Jouberton E, Maubert E, Degoul F, Peyrode C, Chezal JM and Miot-Noirault E. De-

velopment and characterization of a human three-dimensional chondrosarcoma culture for in vitro drug testing. PLoS One 2017; 12: e0181340.
[22] Ziolkowska-Suchanek I. Mimicking tumor hypoxia in non-small cell lung cancer employing three-dimensional in vitro models. Cells 2021; 10: 141.
[23] Bredenoord AL, Clevers H and Knoblich JA. Human tissues in a dish: the research and ethical implications of organoid technology. Science 2017; 355: eaaf9414.
[24] Fatehullah A, Tan SH and Barker N. Organoids as an in vitro model of human development and disease. Nat Cell Biol 2016; 18: 246-254.
[25] Hirschhaeuser F, Menne H, Dittfeld C, West J, Mueller-Klieser W and Kunz-Schughart LA. Multicellular tumor spheroids: an underestimated tool is catching up again. J Biotechnol 2010; 148: 3-15.
[26] Pati F, Gantelius J and Svahn HA. 3D bioprinting of tissue/organ models. Angew Chem Int Ed Engl 2016; 55: 4650-4665.
[27] Teo MY, Rathkopf DE and Kantoff P. Treatment of advanced prostate cancer. Annu Rev Med 2019; 70: 479-499.
[28] Geng H, Xue C, Mendonca J, Sun XX, Liu Q, Reardon PN, Chen Y, Qian K, Hua V, Chen A, Pan F, Yuan J, Dang S, Beer TM, Dai MS, Kachhap SK and Qian DZ. Interplay between hypoxia and androgen controls a metabolic switch conferring resistance to androgen/AR-targeted therapy. Nat Commun 2018; 9: 4972.
[29] Logozzi M, Mizzoni D, Capasso C, Del Prete S, Di Raimo R, Falchi M, Angelini DF, Sciarra A, Maggi M, Supuran CT and Fais S. Plasmatic exosomes from prostate cancer patients show increased carbonic anhydrase IX expression and activity and low pH. J Enzyme Inhib Med Chem 2020; 35: 280-288.
[30] O'Reilly D, Johnson P and Buchanan PJ. Hypoxia induced cancer stem cell enrichment promotes resistance to androgen deprivation therapy in prostate cancer. Steroids 2019; 152: 108497.
[31] Stewart GD, Ross JA, McLaren DB, Parker CC, Habib FK and Riddick AC. The relevance of a hypoxic tumour microenvironment in prostate cancer. BJU Int 2010; 105: 8-13.
[32] Josson S, Matsuoka Y, Chung LW, Zhau HE and Wang R. Tumor-stroma co-evolution in prostate cancer progression and metastasis. Semin Cell Dev Biol 2010; 21: 26-32.
[33] Jing X, Yang F, Shao C, Wei K, Xie M, Shen H and Shu Y. Role of hypoxia in cancer therapy by regulating the tumor microenvironment. Mol Cancer 2019; 18: 157.
[34] Zanoni M, Pignatta S, Arienti C, Bonafe M and Tesei A. Anticancer drug discovery using multicellular tumor spheroid models. Expert Opin Drug Discov 2019; 14: 289-301.
[35] Karlsson H, Fryknas M, Larsson R and Nygren P. Loss of cancer drug activity in colon cancer HCT-116 cells during spheroid formation in a new 3-D spheroid cell culture system. Exp Cell Res 2012; 318: 1577-1585.
[36] Lee JM, Mhawech-Fauceglia P, Lee N, Parsanian LC, Lin YG, Gayther SA and Lawrenson K. A three-dimensional microenvironment alters protein expression and chemosensitivity of epithelial ovarian cancer cells in vitro. Lab Invest 2013; 93: 528-542.
[37] Vinci M, Gowan S, Boxall F, Patterson L, Zimmermann M, Court W, Lomas C, Mendiola M, Hardisson D and Eccles SA. Advances in establishment and analysis of three-dimensional tumor spheroid-based functional assays for target validation and drug evaluation. BMC Biol 2012; 10: 29.
[38] Alvarez-Perez J, Ballesteros P and Cerdan S. Microscopic images of intraspheroidal pH by 1H magnetic resonance chemical shift imaging of pH sensitive indicators. MAGMA 2005; 18: 293-301.
[39] Mahoney BP, Raghunand N, Baggett B and Gillies RJ. Tumor acidity, ion trapping and chemotherapeutics. I. Acid pH affects the distribution of chemotherapeutic agents in vitro. Biochem Pharmacol 2003; 66: 1207-1218.
[40] Thews O, Gassner B, Kelleher DK, Schwerdt G and Gekle M. Impact of hypoxic and acidic extracellular conditions on cytotoxicity of chemotherapeutic drugs. Adv Exp Med Biol 2007; 599: 155-161.
[41] Friedrich J, Eder W, Castaneda J, Doss M, Huber E, Ebner R and Kunz-Schughart LA. A reliable tool to determine cell viability in complex 3-d culture: the acid phosphatase assay. J Biomol Screen 2007; 12: 925-937.
[42] Desoize B and Jardillier J. Multicellular resistance: a paradigm for clinical resistance? Crit Rev Oncol Hematol 2000; 36: 193-207.
[43] Duan JX, Jiao H, Kaizerman J, Stanton T, Evans JW, Lan L, Lorente G, Banica M, Jung D, Wang J, Ma H, Li X, Yang Z, Hoffman RM, Ammons WS, Hart CP and Matteucci M. Potent and highly selective hypoxia-activated achiral phosphoramidate mustards as anticancer drugs. J Med Chem 2008; 51: 2412-2420.
[44] Saggar JK and Tannock IF. Activity of the hypoxia-activated pro-drug TH-302 in hypoxic and perivascular regions of solid tumors and its potential to enhance therapeutic effects of chemotherapy. Int J Cancer 2014; 134: 2726-2734.
[45] Brenner AJ, Floyd J, Fichtel L, Michalek J, Kanakia KP, Huang S, Reardon D, Wen PY and Lee EQ. Phase 2 trial of hypoxia activated evofos-

famide (TH302) for treatment of recurrent bevacizumab-refractory glioblastoma. Sci Rep 2021; 11: 2306.

[46] Borad MJ, Reddy SG, Bahary N, Uronis HE, Sigal D, Cohn AL, Schelman WR, Stephenson J Jr, Chiorean EG, Rosen PJ, Ulrich B, Dragovich T, Del Prete SA, Rarick M, Eng C, Kroll S and Ryan DP. Randomized phase II trial of gemcitabine plus TH-302 versus gemcitabine in patients with advanced pancreatic cancer. J Clin Oncol 2015; 33: 1475-1481.

[47] Baran N and Konopleva M. Molecular pathways: hypoxia-activated prodrugs in cancer therapy. Clin Cancer Res 2017; 23: 2382-2390.

[48] Li Y, Zhao L and Li XF. The hypoxia-activated prodrug TH-302: exploiting hypoxia in cancer therapy. Front Pharmacol 2021; 12: 636892.

[49] Meng F, Evans JW, Bhupathi D, Banica M, Lan L, Lorente G, Duan JX, Cai X, Mowday AM, Guise CP, Maroz A, Anderson RF, Patterson AV, Stachelek GC, Glazer PM, Matteucci MD and Hart CP. Molecular and cellular pharmacology of the hypoxia-activated prodrug TH-302. Mol Cancer Ther 2012; 11: 740-751.

[50] Jayaprakash P, Ai M, Liu A, Budhani P, Bartkowiak T, Sheng J, Ager C, Nicholas C, Jaiswal AR, Sun Y, Shah K, Balasubramanyam S, Li N, Wang G, Ning J, Zal A, Zal T and Curran MA. Targeted hypoxia reduction restores T cell infiltration and sensitizes prostate cancer to immunotherapy. J Clin Invest 2018; 128: 5137-5149.